

Augmented TCR-mediated signaling in infant T cells enables robust responses to respiratory virus infection

Donna Farber (✉ df2396@cumc.columbia.edu)

Columbia University Medical Center <https://orcid.org/0000-0001-8236-9183>

Puspa Thapa

Columbia University

Rebecca Guyer

Columbia University Medical Center

Alexander Yang

Columbia University Medical Center

Christopher Parks

Columbia University Medical Center

Todd M. Brusko

University of Florida <https://orcid.org/0000-0003-2878-9296>

Maigan Brusko

University of Florida

Thomas Connors

Columbia University Irving Medical Center <https://orcid.org/0000-0002-0199-7733>

Article

Keywords: Lung immunity, respiratory infection, Effector differentiation, Infant immunity

Posted Date: February 23rd, 2021

DOI: <https://doi.org/10.21203/rs.3.rs-229370/v1>

License:  This work is licensed under a Creative Commons Attribution 4.0 International License.

[Read Full License](#)

Abstract

Infants require coordinated immune responses to prevent succumbing to multiple infectious challenges, particularly in the respiratory tract. The mechanisms by which infant T cells are functionally adapted for these responses are not well understood. Here, we demonstrate using an *in vivo* co-transfer model that infant T cells generate greater numbers of lung-homing effector cells to influenza infection compared to adult T cells in the same host, due to augmented TCF-1 downregulation and T cell receptor (TCR)-mediated signaling. Importantly, infant T cells show increased sensitivity to low antigen doses, originating at the interface between T cells and antigen-bearing accessory cells—through actin-mediated mobilization of signaling molecules to the immune synapse. This enhanced signaling was also observed in human infant versus adult T cells. Our findings provide a mechanism for how infants control pathogen load and dissemination, important for designing developmentally-appropriate strategies for promoting immune responses at this vulnerable life stage.

Introduction

Newborns and infants are particularly susceptible to morbidity and mortality from ubiquitous viral respiratory tract infections including influenza and respiratory syncytial virus (RSV), compared to adults. Infants also experience recurrent respiratory tract infections due to lack of long-term protective immunity that is well-established in adults^{1, 2}. However, infants and young children can be less susceptible to novel pathogens compared to adults, as manifested in the COVID-19 pandemic; in response to SARS-CoV-2 infection, children exhibit less severe disease, and often are asymptomatic while adults exhibit acute respiratory illness with high mortality in the most severe cases^{3, 4, 5}. Moreover, infants and young children exhibit distinct responses to vaccines compared to adults, although vaccine formulations are the same for all ages^{6, 7}. Understanding the mechanisms for the distinct immune responses to respiratory viruses in early life and childhood is critically important for protecting the most vulnerable of our population from current and emerging pathogens.

The reduced ability of infants to combat viral respiratory infections has been attributed to the immaturity of adaptive immunity mediated by newly developed naïve T cells^{8, 9}. However, recent studies show that infant immune responses to infection are not necessarily of lower magnitude compared to adults, but rather exhibit distinct functional features and altered T cell differentiation fates^{10, 11}. In response to systemic and respiratory virus infection, infant CD8⁺ and CD4⁺ T cells exhibit enhanced proliferation and/or differentiation to effector cells, and reduced memory formation¹². These distinct responses of neonatal T cells derive in part, from their maturation from fetal progenitors compared to T cells generated during the post-natal period, resulting in altered transcriptional profiles^{13, 14}. The induction and expression levels of the transcription factor T-bet can bias effector over memory T cell fate in adult mouse T cells, and we previously showed that reducing T-bet expression in infant T cells reduced effector generation *in vivo*^{12, 15}, demonstrating similar regulation of effector cell fate in infant T cells. Another transcription factor determining T cell fate, TCF-1, is required for memory formation and inhibits effector formation¹⁶,

^{17, 18}, though its role in infant T cell differentiation is not known. Moreover, the upstream mechanisms driving differential activation and fate determination in infant T cells remains unclear.

Antigen-mediated activation of T cells triggers T cell-receptor (TCR)-coupled signaling events which lead to transcription factor activation. T cell activation begins with the formation of an immune synapse (IS) between the T cell and antigen presenting cell (APC) which contain the molecular contact points between the TCR, Ag/MHC, the CD4 or CD8 co-receptor, and integrins such as LFA-1 (CD11a)¹⁹. IS formation and maintenance is essential for initiation and propagation of proximal signaling events including phosphorylation of CD3 chains by the co-receptor-coupled p56Lck tyrosine kinase, thereby governing the magnitude of TCR-mediated signaling^{20, 21, 22}. TCR signal strength also influences differentiation with stronger TCR signal strength biasing effector differentiation over memory T cell fate^{23, 24, 25}. The role of these earliest events in T cell activation and TCR-coupled signaling in specific responses of infant T cells is not known.

In this study, we investigated the molecular mechanisms for the distinct responses to infant compared to adult T cells in mice and humans. Using a co-transfer model to track the intrinsic activation properties of infant and adult T cells in the same host to respiratory infection, we found that virus-specific infant T cells exhibited increased proliferation and generation of lung-homing effector T cells along with reduced TCF-1 expression compared to adult T cells in the same host. These distinct infant T cell responses were upstream of transcription factor induction, and were due to enhanced IS formation and proximal TCR signaling by infant compared to adult T cells in response to antigen. This enhanced TCR signaling leading to reduced activation threshold and TCF-1 downregulation, was recapitulated in human infant T cells. Our findings demonstrate that infant T cells exhibit enhanced signaling to combat multiple antigenic challenges of early life, with implications for the design of age-targeted strategies for boosting immunity in this critical life stage.

Results

Enhanced generation of lung-homing effector cells by infant compared to adult T cells during respiratory virus infection

To study intrinsic properties of infant versus adult T cells to influenza infection, we established a co-transfer model to follow the fate of infant or adult-derived influenza-specific CD4⁺ T cells *in vivo* in multiple tissue sites within the same host. Infant T cells were obtained from mice 10–14 days old previously shown to be the timepoint where mouse neonatal T cells are most similar in phenotype to human infant naïve T cells¹², while adult T cells were obtained from mice 6–8 weeks of age or older. We transferred equal numbers of CD4⁺ T cells from infant and adult OT-II TCR transgenic mice, expressing a transgene-encoded TCR specific for chicken ovalbumin²⁶, into congenic adult mouse hosts, which were subsequently infected with recombinant influenza virus expressing the OT-II-specific epitope (PR8-OVA, Fig. 1a). Differential expression of congenic markers was used to distinguish between transferred infant, adult, and host T cells in the lung and lung-draining mediastinal lymph node (medLN) at indicated times

post-infection. Prior to infection, the frequencies of infant and adult OT-II cells in host LN were equivalent (Fig. 1b), indicating comparable persistence after transfer.

T cell responses to influenza virus are typically primed in the medLN where they develop into lung-homing effector cells which direct lung viral clearance *in situ*^{27, 28}. At early times post-infection, (day 4 p.i.) there was significantly higher proportion of infant compared to adult T cells in the medLN (Fig. 1c), which also exhibited increased proliferation compared to adult T cells (Fig. 1c-d). Few undivided OT-II cells (infant or adult origin) had migrated to the lungs at this early time point (Supplementary Fig. 1a). During the peak T cell response (day 7–15 p.i.) infant T cells predominated over adult T cells in the lungs by frequency and absolute numbers—outnumbering adult cells by 4:1—but were present in comparable frequency and numbers to adult T cells in the mediastinal lymph nodes at these time points (Fig. 1e-g). Infant OT-II T cells in the lungs also had a higher frequency of effector cells producing the pro-inflammatory cytokines IFNy and TNFa compared to adult lung OT-II cells (Fig. 1h). These findings show that infant T cells are enhanced compared to adult T cells in their capacity to proliferate and differentiate into lung-homing effector cells in response to respiratory virus infection.

Infant T cells downregulate TCF-1 for enhanced proliferation but not effector generation.

T cell proliferation and effector differentiation is regulated by expression of transcription factors TCF-1 and T-bet, respectively^{29, 30, 31}. T-bet expression was elevated in lung-homing effector OT-II cells compared to host naïve T cells (Supplementary Fig. 2a), and there were increased numbers of T-bet^{hi} infant-compared to adult-derived lung OT-II T cells (Fig. 1f, Supplementary Fig. 2b). These results confirm that infant T cells exhibit enhanced differentiation to lung-homing effector cells as we previously showed in infant versus adult mice infected with influenza¹². In contrast to T-bet, TCF-1 is required for self-renewal, is highly expressed in naïve T cells, and is downregulated during effector differentiation while memory precursor T cells retain TCF-1 expression^{16, 32}. Prior to infection, infant OT-II cells exhibited similar high levels of TCF-1 compared to adult cells (Supplementary Fig. 2c). However, by day 4 p.i. TCF-1 expression was downregulated in proliferating infant T cells (CPD^{lo}) in the medLN, to a greater extent than in proliferating adult T cells; non-dividing (CPD^{hi}) infant and adult T cells had comparably high TCF-1 expression (Fig. 2a). Reduced TCF-1 expression by infant T cells was also observed in lung homing effector T cells at day 7–15 p.i.; adult lung OT-II cells had significantly higher TCF-1 expression compared to infant lung OT-II cells (Fig. 2b). Together, these finding show that the enhanced expansion and lung homing of infant T cells is accompanied by an early and more rapid downregulation of TCF-1 compared to adult CD4⁺ T cells.

To assess whether if maintaining TCF-1 expression in infant T cells would reduce their proliferative and/or lung homing capacities to similar levels as adult T cells, we generated OT-II mice with fixed expression of TCF-1 by crossing to a TCF-1 transgenic (p45-Tg) strain³³. Similar co-transfers were set up as in Fig. 1, with equal numbers of infant OT-II/TCF-1 Tg and adult OT-II T cells transferred into congenic hosts followed by PR8-OVA challenge. Prior to virus challenge, there were comparable frequencies of

infant and adult T cells in the LN with infant OT-II/TCF-1 Tg T cells expressing higher levels of TCF-1 compared to adult WT OT-II (Fig. 2c). Following PR8-OVA challenge, the frequency and number of infant OT-II/TCF-1 Tg effector T cells was similar to adult OT-II effector T cells in the lungs but reduced compared to adult OT-II cells in the medLN (Fig. 2d, Supplemental Fig. 2d). While the ratio of infant: adult OT-II cells in the lung was comparable there was a reduced frequency and numbers of infant OT-II/TCF-1 compared to adult OT-II cells in the medLN (Fig. 2e). These findings show that although the overall number of expanded infant T cells was reduced when TCF-1 expression was restored, infant T cells were still biased towards effector generation and lung homing. These results indicate that the mechanisms driving enhanced effector generation of infant T cells were upstream of TCF-1 expression.

Enhanced TCR-mediated signaling by infant T cells *in vivo*

We hypothesized that the enhanced effector differentiation by infant T cells could be driven by the earliest events of T cell activation and signaling. To measure the extent of TCR-mediated signaling to influenza infection *in vivo* in the co-transfer model, we assessed two parameters: 1. surface expression of the OT-II TCR using a specific tetramer³⁴, as programmed downregulation of the TCR correlates with TCR signal strength³⁵, and 2. expression of CD5 following activation which correlates with TCR affinity for its antigen^{36,37}. Both infant and adult OT-II cells in LNs had comparable expression of the OT-II TCR and CD5 prior to influenza challenge (Fig. 3a, b). Following influenza challenge, however, infant lung effector OT-II cells had significantly reduced TCR and CD5 expression compared to adult effector OT-II cells at the peak timepoints for lung T cell responses (Fig. 3a, b). This shift to reduced TCR and CD5 expression by infant OT-II cells relative to adult OT-II also occurred in infant TCF-1 Tg cells (Fig. 3c, d), further indicating that events are upstream of TCF-1-mediated transcriptional events. The presence of significantly reduced CD5 expression in infant compared to adult effector cells (Fig. 3b,d) could be due to loss of the CD5hi-expressing high affinity infant T cells^{38,39}. Indeed, infant effector T cells exhibited higher apoptotic frequencies by Annexin V staining compared to adult effector T cells (Supplementary Fig. 3), suggesting increased activation induced cell death (AICD) due to higher TCR signal strength. Together, these data indicate that enhanced TCR signaling independent of TCF-1 activity is a distinct response employed by infant T cells.

Enhanced TCR sensitivity by infant T cells lowers the activation threshold

We hypothesized that enhanced TCR signaling as manifested *in vivo* by increased TCR downregulation would lead to enhanced sensitivity of infant T cells to antigenic stimulation. We stimulated infant and adult OT-II T cells with varying doses of OVA peptide antigen and assessed multiple readouts for functional and transcriptional responses at different time points. Infant OT-II cells exhibit increased and more rapid proliferative responses to lower peptide doses (0.01-0.1µg) compared to adult OT-II cells (Fig. 4a). Infant T cells also expressed higher levels of activation markers CD69 and CD25 at a lower peptide dose that was not sufficient for induction of these markers by adult T cells (Fig. 4b), despite equivalent surface expression of the OT-II shown above (Fig. 3a). Moreover, there was significantly higher induction of key transcription factors Nur77 and IRF4 which are directly downstream of TCR signaling⁴⁰,

⁴¹ by infant T cells compared to adult T cells at the low and intermediate antigen doses (Fig. 4c). These results demonstrate a dramatically higher antigen sensitivity and reduced activation threshold for infant T cells compared to adult T cells, suggesting that infant T cells are more adapted for responses in conditions of limited antigen availability.

Increased TCR-coupled proximal signaling by infant compared to adult T cells

In order to investigate the mechanisms by which infant T cells exhibit enhanced signaling and TCR sensitivity despite equivalent TCR levels at baseline, we examined early manifestations of TCR signaling within minutes to hours following antigen-mediated stimulation. Infant OT-II cells exhibited more rapid kinetics of surface TCR- β downmodulation compared to adult OT-II cells, starting at 2hrs post-stimulation and was reduced further up to 8hrs post-stimulation (Fig. 5a). Compared to adult T cells, infant T cells also showed a more rapid and enhanced upregulation of Nur77 expression, an orphan nuclear receptor which is a marker of early TCR-mediated signaling^{42, 43, 44} (Fig. 5b). Early signaling events more proximal to Nur77 were also augmented in infant T cells, such as phosphorylation of ERK1/2, a proximal signaling event that occurs following activation of TCR-coupled tyrosine kinases⁴⁵. An increased proportion of infant CD4 $^{+}$ T cells phosphorylated erk1/2 at earlier times following TCR engagement, compared to adult CD4 $^{+}$ T cells (Fig. 5c). These results indicate that infant CD4 $^{+}$ T cells have an increased intrinsic capacity for enhanced proximal TCR-coupled signaling compared to adult T cells responding to the same antigenic epitope.

Infant T cells more readily form immunological synapses with antigen-bearing accessory cells

TCR activation and early signaling are triggered when the TCR and accessory molecules, bind their respective ligands on the surface of an antigen presenting cell (APC) forming an immunological synapse (IS) at the point of contact^{19, 20}. Key molecules in the mature IS include LFA-1(CD11a), an integrin for stable conjugate formation, actin for overall mobilization of signaling molecules to the TCR, and p56lck kinase, an essential tyrosine kinase coupled to the CD4 and CD8 co-receptors^{46, 47, 48}. To determine if the distinct TCR signaling capacity of infant compared to adult T cells is regulated at the level of IS formation, we employed imaging flow cytometry to visualize T cells in contact with APC^{49, 50} and key molecules associated with IS formation in the presence or absence of the antigenic stimulus (see methods). OT-II cells and APCs were distinguished by differential fluorescent labeling as well as expression of surface and intracellular markers expressed by each cell and in the contact zone between them (Fig. 6a).

Unstimulated infant and adult T cells expressed comparable levels of CD3 ϵ , CD4, intracellular Lck, and LFA-1 (Supplemental Fig. 4a) and did not form IS when present in conjugates with APC in the absence of antigen, as manifested by the broad distribution of CD3 and actin around the cell perimeter (Fig. 6b). Upon stimulation with cognate antigen, bright staining of CD3 ϵ with the integrin LFA-1, and CD3 ϵ with actin were observed inside the zone of contact between the T cell and the APC for infant and adult T cells within 10 minutes and maintained through 60 minutes indicating stable IS formation (Supplemental Fig. 4b, Fig. 6b). While quantitative accumulation of LFA-1 within the IS was similar between infant and

adult T cells (Supplemental Fig. 4b), there were significantly higher levels of actin in the IS of infant compared to adult OT-II cells at all timepoints (Fig. 6b, right). Because actin regulates organization of signaling molecules to the IS^{46, 51}, we assessed the level of CD4-coupled p56lck within the IS. Both p56lck and CD4 showed significantly higher accumulation within the IS of infant compared to adult T cells starting at 10 min and maintained through 60 min of stimulation (Fig. 6c, d). Together, these findings indicate that increased TCR-coupled signaling by infant compared to adult T cells originates at the earliest stage in T cell activation—through actin-mediated mobilization of signaling molecules to the IS.

Human infant T cells exhibit enhanced TCR-coupled signaling and TCF-1 downregulation

To address if human infant T cells exhibit similar enhancements in TCR-coupled signaling and differentiation compared to adult T cells, we examined the response of purified naïve CD4⁺ T cells isolated from infant and adult lymph node T cells to activation by anti-CD3/anti-CD28/anti-CD2-coupled beads, as surrogates for an antigen-driven response. Human naïve T cells upregulated Nur77 within hours of stimulation, with infant T cells showing higher levels of Nur77 expression compared to their adult counterparts (Fig. 7a). Human infant T cells also have reduced capacity to retain TCF-1 expression following stimulation and proliferation compared to adult T cells (Fig. 7b). This enhanced downregulation of TCF-1 expression by human infant T cells suggests biased effector differentiation. These results indicate that human naïve T cells also show age-dependent potencies in TCR-mediated activation; those derived early in life have an enhanced capacity for TCR-coupled signaling driving enhanced effector differentiation compared to naïve T cells which persist in adults.

Discussion

Infants are predisposed to complications from respiratory infections, particularly for ubiquitous pathogens such as influenza and RSV for which older children and adults have developed long-term immunity. While it has been shown that T cells exhibit altered functional responses during infancy^{9, 12, 13, 14}, basic mechanism for these distinct responses remain incompletely understood. In this study, we demonstrate using an *in vivo* model of influenza infection, *ex vivo* signaling and functional analyses, and coordinate assays in mice and humans, that infant T cells are intrinsically adapted to mediate augmented responses due to increased TCR-coupled signaling originating at the most proximal stage of T cell activation—IS formation. This enhanced TCR-coupled signaling results in an intrinsic bias for differentiation to tissue-homing effector cells that governs their response to multiple new antigen encounters during this unique period of exposure and immune education. Our findings can help inform developmentally-appropriate strategies for promoting immunity at this early life stage.

We used a co-transfer model of infant and adult TCR transgenic OT-II T cells recognizing a single antigenic epitope within a recombinant influenza strain, to enable direct comparison of antigen-specific responses to infection that were intrinsic to infant or adult T cells. Importantly, infant virus-reactive T cells exhibited robust proliferation to influenza infection, out-pacing expansion of adult-derived T cells and predominating over them in the lung. This expansion was accompanied by downmodulation of the transcription factor TCF-1 to a greater extent in infant compared to adult T cells, consistent with the

known reduction in TCF-1 expression during proliferative expansion and effector differentiation^{16, 29}. However, fixed expression of TCF-1 in infant T cells, while it constrained infant T cell proliferation to similar levels as adults, TCF-1-tg infant T cells still exhibited biased lung homing compared to adult T cells, indicating signals upstream of TCF-1 activity were regulating distinct responses in infants. These upstream TCF-1-independent processes in infant T cells occurred at the level of TCR-mediated signal transduction.

Our upstream analyses revealed that the distinct responses of infant T cells to infection originate at the earliest stage of T cell activation during IS formation. The initial discovery of the IS provided evidence for structural organization of the T cell-APC conjugate as a critical requirement for TCR-coupled signaling and subsequent activation outcomes^{20, 21, 46}. Infant T cells generate mature IS with increased kinetics compared to adult T cells and mobilize greater quantities of actin and CD4-coupled p56lck to the IS, despite expressing comparable levels of these molecules and the same TCR as adult cells. As the cytoskeleton and membrane dynamics can affect IS formation^{21, 51}, differences in membrane fluidity or structure of infant T cells may facilitate their interaction with APC. Further investigation of the biophysical properties of infant relative to adult T cells may provide additional insight into this process.

The specific responses of infant T cells may derive from their origin and/or recent emergence from the thymus. Rudd and colleagues showed that neonatal T cells present at birth are derived from fetal bone marrow progenitors and these T cells have distinct transcriptional profiles compared to T cells generated postnatally¹³. For our studies, we obtained T cells at later stages of infancy in mice, allowing for 10–14 days of post-natal development and we show similar enhanced signaling in human T cells up to 2 years of age. Mouse models examining recent thymic emigrants (RTE) marked by green fluorescent protein (GFP) expression also identified enhanced proliferation and responses by RTE compared to naïve T cells which persisted in the periphery⁵². While these results suggest that some of the findings may be due to newly developed naïve T cells, RTE were also found to be impaired in effector and proinflammatory cytokine production^{52, 53}, unlike infant T cells examined here. Together, our findings suggest that developmental origin and “newness” may contribute to the distinct activation properties of infant T cells, in addition to other factors.

The higher TCR-coupled signaling strength of infant T cells results in increased sensitivity to low antigen doses compared to adult T cells. The ability of infants to generate adaptive immune responses to minute levels of antigen, could facilitate protection from viruses which replicate exponentially in the host. Enhanced TCR signaling could also explain the advantage of infants and young children in generating efficacious primary responses to novel pathogens, like SARS-CoV-2 which rarely infects infants and exhibits reduced infection and dissemination in children compared to adults^{3, 4, 5}. Higher sensitivity T cell responses can promote clearance of low viral doses, preventing viral replication and dissemination to pathogenic levels as seen in adults. Whether this enhanced sensitivity of infant T cells in humans is maintained throughout childhood remains to be determined, though recent evidence shows distinct immune responses for children of all ages compared to adults to respiratory challenge³. Future studies

comparing virus-reactive T cells in young children and adults can provide insights into the anti-viral immunity at different life stages.

Vaccines can hasten the establishment of long-term immunity when administered in early life; however, optimizing immune responses involves modulating the formulation, dose or administration in a developmentally appropriate manner. Our results suggest that use of lower doses and/or moving up vaccination to earlier times post-natally may promote immune responses to diverse pathogens. Such age-targeted strategies for immune enhancement can prevent serious disease and provide immune education for current and future pathogens at this formative life stage.

Methods And Materials

Mice

Mice were housed and bred in specific pathogen-free (Spf) conditions in the animal facilities at Columbia University Irving Medical Center (CUIMC). OT-II (B6.Cg.Tg(TcraTcrb)425Cbn/J)²⁶ and CD45.1(B6.SJL-Ptprc^aPepc^b/BoyJ) mice were purchased from Jackson Laboratories while C57BL/6 mice were purchased from Charles River. TCF-1 (p45) transgenic mice expressing the long isoform of TCF-1³³ were generously provided by Dr. Hai-Hui Xue and Dr. Werner Held. CD45.1 mice were bred to generate CD45.1 congenic hosts and CD45.2 mice were bred to use for phosphoflow studies. OT-II mice were also crossed to CD45.1 mice and TCF-1 Tg OT-II mice were generated by breeding TCF-1 Tg male to OT-II females. All infant mice were used at 10–14 days of age, and adult mice were used at 6 weeks and older. Infections were performed in BSL-2 level biocontainment animal facilities. All animal studies were approved by Columbia University IACUC.

T cell adoptive transfer and Influenza infection

To isolate CD4 T cells from infant and adult mice, spleen and lymph nodes were harvested and processed to generate a single cell suspension. Single litters of at least 5 pups were combined to generate sufficient numbers of CD4⁺ T cells for each experiment. CD4 T cells were purified by negative magnetic selection (Stemcell Technologies, Cambridge, MA). For co-transfers, 250,000 cells in 100 μ l of PBS containing 1:1 ratio of adult and infant OT-II T cells were transferred into adult congenic B6 or CD45.1 host mice retro-orbitally one-day prior (day – 1) to infection. For 4-day *in vivo* proliferation experiments, OT-II T cells were labeled with cell proliferation dye (CPD) (ThermoFisher) and 500,000 each of infant and adult T cells were transferred into host mice. At day 0, host mice were infected intranasally (i.n.) with 2000 TCID₅₀ of a recombinant PR8-OVA strain expressing the OVA323–339 peptide (sequence ISQAVHAAHAEINEAGR; provided by Dr. Paul Thomas, St. Jude Children's Research Hospital, Memphis, TN)⁵⁴.

Flow cytometry

Mediastinal lymph nodes and lungs were harvested at indicated days of infections and processed to generate single cell suspension as previously described^{12, 55}. A list of all antibodies used for flow

cytometry in this study is in Supplemental Table 2. In general, cells were first stained with surface markers at 30 min room temperature (RT) and an additional 30 min on ice. Cells were then fixed and permeabilized with FoXP3 fix/perm (Tonbo) before being stained for intracellular markers for 30 min on ice. For OTII TCR specific tetramer staining, cells were incubated with I-A(b)_{AAHAEINEA} tetramers in 50 μ L for 1hr in 37°C incubator before addition of other surface markers with additional 30 min at RT before fixation as described above. For Annexin V staining, cells were stained for surface markers and washed before staining for Annexin V for 20 min at RT. Cells were washed and quickly analyzed in a cytometer. All flow cytometry samples were acquired using LSRII cytometry (BD) with FACSDiva software. All cell sorting were performed in BD Influx cell sorter. Data were analyzed using FSC Express (DeNovo software).

Human donor samples

Human adult lymph nodes were obtained from deceased (brain dead) organ donors through an approved protocol and material transfer agreement with LiveOnNY as described⁵⁶. Human infant lymph nodes were obtained from deceased (brain dead) organ donors under the Human Atlas for Neonatal Development and Early Life – Immunity (HANDEL-I) tissue procurement program. A list of all donors used and their ages is in Supplemental Table 1. Tissues were obtained and processed for single-cell suspensions, as previously described⁵⁷. The study does not qualify as human subjects research as determined by Columbia University institutional review board (IRB), because tissue samples were obtained from deceased individuals.

Mouse T cell stimulations

For activation of OT-II CD4 $^{+}$ T cells, OT-II cells were isolated from spleens and LNs of infant and adult mice as described above, labeled with CPD and cultured 1:1 with antigen presenting cells (APC; T-depleted splenocytes from adult CD45.1 or C57BL/6 mice in the presence of chicken ovalbumin peptide epitope recognized by the OT-II TCR (ISQAVHAAHAEINEAGR) (InVivoGen) in complete RPMI media (10% fetal bovine serum (FBS), 1% penicillin – streptomycin-glutamine (PSQ), 25mM HEPES). Controls were T cell and APC cultured without peptide. For short-term stimulations for assessing TCR signaling, infant or adult OT-II cells were stimulated with 10 μ g of peptide-pulsed T cell-depleted splenocytes. For measuring cytokine production by lung T cells, total lung cells were isolated as described^{12, 55} from mice at day 11 post-infection and stimulated in the presence of 10 μ g of peptide for 6–16 hr in complete RPMI. Protein transport inhibitor (ThermoFisher) was added 2 hours into stimulation. After stimulation cells were first stained with surface markers, then fixed and permeabilized with FoXP3 fix/perm (Tonbo) before being stained for intracellular cytokine for 30 min on ice.

Human T cell stimulation.

Naïve (CD45RA $^{+}$ CCR7 $^{+}$) CD4 $^{+}$ T cells were sorted from lymph nodes (LN), labeled with cell proliferation dye (CPD), and allowed to rest overnight before stimulation. Cells (100,000 cells/well) were cultured with carboxylate modified latex (CML) microbeads (ThermoFisher) functionalized with 10 μ g/mL of anti-CD28

(BioXcell) and anti-CD2 (ThermoFisher) monoclonal antibodies and 0.1–10 μ g/mL of anti-CD3 monoclonal antibody (BioXcell), at 1:1 in complete AIM V media (10% human serum, 1% PSQ, Glutamax, and IL-2 (50ng/ml)). Preparation of CML microbeads used for stimulation was done as described ^{58, 59, 60}.

For short-term (0-8hr) stimulation, total lymph node T cells were pre-stained with surface makers CD4, CD3, CD45RA, and CCR7 before being plated in complete RPMI media. Cells were stimulated using beads coated with 10 μ g/mL of anti-CD3/ anti-CD28/ anti-CD2 (Miltenyi) for indicated time. At each time point, cells were harvested and further stained for surface marker (CD3) before being fixed and permeabilized for intracellular marker Nur77.

TCR signaling analysis using Phosphoflow

C57BL/6 wild-type (WT) mice were used for examination of phosphoERK1/2 expression upon stimulation. Cells were isolated with magnetic negative enrichment using CD3 isolation kit (StemCell). CD3 enriched cells were kept ice cold until time of stimulation in 37°C water bath. Cells were first labeled with anti-CD3 ϵ (10 μ g/ml) and anti-CD28 (5 μ g/ml) (BioXcell) antibodies in ice cold PBS for 30min on ice. Cells were washed and then stained with cross-linker goat anti-Armenian hamster IgG (Jackson Immuno Research Laboratories) (20 μ g/ml) and anti-CD44/ anti-CD62L antibodies for additional 30min on ice. Tubes were then placed in water bath to start stimulation and lyse/fix buffer (BD) was added to stop stimulation at indicated times. Cells were permeabilized with Perm III buffer (BD) before being stained for CD3, CD4, CD8, and pERK1/2.

Analysis of T cell and APC conjugates

To image immunological synapse (IS) formation between OT-II T cells and APC, CPD labeled OT-II cells were pre-stained with anti-CD4 antibodies at 4°C and washed with ice cold PBS before stimulation. OT-II cells were then placed with 10 μ g of peptide pulsed T cell-depleted CFSE-labeled splenocytes and spun down at 100 x g for 1min to enable conjugation. Stimulation was started by placing tubes into 37°C water bath. After each stimulation time point, cells were fixed with cytofix (BD) and placed on ice overnight. Next day, cells were washed and then permeabilized with 1x Triton-X solution (Sigma-Aldrich) for 15min RT. After wash, cells were stained with the rest of the markers in RT before being analyzed by ImageStream X (Amnis, Seattle, WA).

Image stream analysis

Images were acquired at 60x magnification on a four-laser ImageStream X (Amnis, Seattle, WA) imaging flow cytometer with INSPIRE software. Data was analyzed using IDEAS v6. Using Area measurement, doublet cells were gated and acquired for all samples. From doublet cells, events with both CPD and CFSE dye were gated to identify conjugates of T cell: APC. Previously published analysis from Au-Wabnitz et al and Abrahamsen et al was adapted ^{49, 50}. Using the ‘threshold’ mask function on CPD channel, T cell were highlighted. With ‘interface’ mask function on CPD, the immune synapse of T cells was highlighted. Formula used to quantify accumulation of molecules in the IS:

$$\text{percent accumulation} = \frac{\text{intensity in IS}}{\text{intensity in T cell}} \times 100$$

To adjust for background differences existing before stimulation, quantification was normalized to unstimulated controls.

Statistical analysis

All data were compiled and statistical analysis performed using Prism software (GraphPad Software). Results are shown with SEM unless otherwise indicated. Significance was determined using Student's *t*-test or two-way repeated measure ANOVA with multiple comparison testing using the Sidak method. Result was designated significant when *p* value was *p* ≤ 0.05.

Abbreviations

MedLN – Mediastinal Lymph Node; TCR – T Cell Receptor; IS – Immune Synapse; TCF-1 – T Cell Factor 1, APC – Antigen Presenting Cell, MHC – Major Histocompatibility Complex

Declarations

AUTHOR CONTRIBUTIONS

P.T. designed and performed experiments, analyzed data, and wrote the manuscript; R.S.G. and A.Y. performed experiments and analyzed data. C.A.P. designed experiments and analyzed data. T.B. and M.B. coordinated acquisition of human infant tissues. T.C. coordinated acquisition and processing of human infant tissue. D.L.F planned experiments, analyzed data, wrote and edited the manuscript.

ACKNOWLEDGEMENTS

This work was supported by NIH grant AI100119 awarded to D.L.F. T.J.C. was supported by K23 AI141686 and T.M.B was supported by AI42288. These studies were performed in the CCTI Flow Cytometry Core supported by NIH S10RR027050 and S10OD020056. Acquisition of human samples from the University of Florida was supported by the Helmsley Charitable Trust (to T.M.B. and D.L.F.) ImageStream experiments were performed in Columbia Stem Cell initiative (CSCI) Flow Core, supported in part by NIH (S10OD026845). We are grateful to Werner Held, University of Lausanne, and Hai-Hui Xue, University of Iowa, for their generosity in providing the TCF-1 (p45) Tg mice.

We wish to thank Stuart Weisberg for reviewing the manuscript and his helpful comments and discussion.

References

1. Mohr, E. & Siegrist, C.-A. Vaccination in early life: standing up to the challenges. *Current Opinion in Immunology* **41**, 1–8 (2016).
2. PrabhuDas, M. *et al.* Challenges in infant immunity: implications for responses to infection and vaccines. *Nat Immunol* **12**, 189–194 (2011).
3. Weisberg, S.P. *et al.* Distinct antibody responses to SARS-CoV-2 in children and adults across the COVID-19 clinical spectrum. *Nature Immunology* **22**, 25–31 (2021).
4. Alsohime, F., Temsah, M.-H., Al-Nemri, A.M., Somily, A.M. & Al-Subaie, S. COVID-19 infection prevalence in pediatric population: Etiology, clinical presentation, and outcome. *J Infect Public Health* **13**, 1791–1796 (2020).
5. Barrero-Castillero, A. *et al.* COVID-19: neonatal–perinatal perspectives. *Journal of Perinatology* (2020).
6. Alexander-Miller, M.A. Challenges for the Newborn Following Influenza Virus Infection and Prospects for an Effective Vaccine. *Frontiers in immunology* **11**, 568651–568651 (2020).
7. PrabhuDas, M. *et al.* Challenges in infant immunity: implications for responses to infection and vaccines. *Nature Immunology* **12**, 189–194 (2011).
8. Schmiedeberg, K. *et al.* T Cells of Infants Are Mature, but Hyporeactive Due to Limited Ca²⁺ Influx. *PloS one* **11**, e0166633–e0166633 (2016).
9. Pichichero, M.E. *et al.* Functional Immune Cell Differences Associated With Low Vaccine Responses in Infants. *The Journal of Infectious Diseases* **213**, 2014–2019 (2016).
10. Davenport, M.P., Smith, N.L. & Rudd, B.D. Building a T cell compartment: how immune cell development shapes function. *Nat Rev Immunol* **20**, 499–506 (2020).
11. Rudd, B.D. Neonatal T Cells: A Reinterpretation. *Annu Rev Immunol* **38**, 229–247 (2020).
12. Zens, K.D. *et al.* Reduced generation of lung tissue-resident memory T cells during infancy. *The Journal of experimental medicine* **214**, 2915–2932 (2017).
13. Smith, N.L. *et al.* Developmental Origin Governs CD8 + T Cell Fate Decisions during Infection. *Cell* **174**, 117–130.e114 (2018).
14. Smith, N.L. *et al.* Rapid proliferation and differentiation impairs the development of memory CD8 + T cells in early life. *J Immunol* **193**, 177–184 (2014).
15. Joshi, N.S. *et al.* Inflammation directs memory precursor and short-lived effector CD8(+) T cell fates via the graded expression of T-bet transcription factor. *Immunity* **27**, 281–295 (2007).
16. Zhou, X. *et al.* Differentiation and persistence of memory CD8(+) T cells depend on T cell factor 1. *Immunity* **33**, 229–240 (2010).
17. Yu, Q. *et al.* T cell factor 1 initiates the T helper type 2 fate by inducing the transcription factor GATA-3 and repressing interferon-gamma. *Nat Immunol* **10**, 992–999 (2009).
18. Nish, S.A. *et al.* CD4 + T cell effector commitment coupled to self-renewal by asymmetric cell divisions. *The Journal of experimental medicine* **214**, 39–47 (2017).

19. Monks, C.R.F., Freiberg, B.A., Kupfer, H., Sciaky, N. & Kupfer, A. Three-dimensional segregation of supramolecular activation clusters in T cells. *Nature***395**, 82–86 (1998).
20. Dustin, M.L. T-cell activation through immunological synapses and kinapses. *Immunological Reviews***221**, 77–89 (2008).
21. Grakoui, A. *et al.* The Immunological Synapse: A Molecular Machine Controlling T Cell Activation. *Science***285**, 221 (1999).
22. Li, Q.-J. *et al.* CD4 enhances T cell sensitivity to antigen by coordinating Lck accumulation at the immunological synapse. *Nature Immunology***5**, 791–799 (2004).
23. King, Carolyn G. *et al.* T Cell Affinity Regulates Asymmetric Division, Effector Cell Differentiation, and Tissue Pathology. *Immunity***37**, 709–720 (2012).
24. Cho, Y.-L. *et al.* TCR Signal Quality Modulates Fate Decisions of Single CD4 + T Cells in a Probabilistic Manner. *Cell Reports***20**, 806–818 (2017).
25. Snook, J.P., Kim, C. & Williams, M.A. TCR signal strength controls the differentiation of CD4(+) effector and memory T cells. *Sci Immunol***3** (2018).
26. Barnden, M.J., Allison, J., Heath, W.R. & Carbone, F.R. Defective TCR expression in transgenic mice constructed using cDNA-based α - and β -chain genes under the control of heterologous regulatory elements. *Immunology & Cell Biology***76**, 34–40 (1998).
27. Paik, D.H. & Farber, D.L. Influenza infection fortifies local lymph nodes to promote lung-resident heterosubtypic immunity. *Journal of Experimental Medicine***218** (2020).
28. Ho, A.W. *et al.* Lung CD103 + dendritic cells efficiently transport influenza virus to the lymph node and load viral antigen onto MHC class I for presentation to CD8 T cells. *J Immuno***187**, 6011–6021 (2011).
29. Nish, S.A. *et al.* CD4 + T cell effector commitment coupled to self-renewal by asymmetric cell divisions. *Journal of Experimental Medicine***214**, 39–47 (2016).
30. Lin, W.-H.W. *et al.* CD8(+) T Lymphocyte Self-Renewal during Effector Cell Determination. *Cell reports***17**, 1773–1782 (2016).
31. Szabo, S.J. *et al.* A Novel Transcription Factor, T-bet, Directs Th1 Lineage Commitment. *Cell***100**, 655–669 (2000).
32. Danilo, M., Chennupati, V., Silva, J.G., Siegert, S. & Held, W. Suppression of Tcf1 by Inflammatory Cytokines Facilitates Effector CD8 T Cell Differentiation. *Cell Reports***22**, 2107–2117 (2018).
33. Ioannidis, V., Beermann, F., Clevers, H. & Held, W. The β -catenin–TCF-1 pathway ensures CD4 + CD8 + thymocyte survival. *Nature Immunology***2**, 691–697 (2001).
34. Landais, E. *et al.* New Design of MHC Class II Tetramers to Accommodate Fundamental Principles of Antigen Presentation. *The Journal of Immunology***183**, 7949 (2009).
35. Gallegos, A.M. *et al.* Control of T cell antigen reactivity via programmed TCR downregulation. *Nature Immunology***17**, 379–386 (2016).

36. Fulton, R.B. *et al.* The TCR's sensitivity to self peptide-MHC dictates the ability of naive CD8(+) T cells to respond to foreign antigens. *Nature immunology***16**, 107–117 (2015).
37. Persaud, S.P., Parker, C.R., Lo, W.-L., Weber, K.S. & Allen, P.M. Intrinsic CD4 + T cell sensitivity and response to a pathogen are set and sustained by avidity for thymic and peripheral complexes of self peptide and MHC. *Nature immunology***15**, 266–274 (2014).
38. Azzam, H.S. *et al.* CD5 expression is developmentally regulated by T cell receptor (TCR) signals and TCR avidity. *J Exp Med***188**, 2301–2311 (1998).
39. Weber, K.S. *et al.* Distinct CD4 + helper T cells involved in primary and secondary responses to infection. *Proc Natl Acad Sci U S A***109**, 9511–9516 (2012).
40. Moran, A.E. *et al.* T cell receptor signal strength in Treg and iNKT cell development demonstrated by a novel fluorescent reporter mouse. *The Journal of experimental medicine***208**, 1279–1289 (2011).
41. Nayar, R. *et al.* TCR signaling via Tec kinase ITK and interferon regulatory factor 4 (IRF4) regulates CD8 + T-cell differentiation. *Proc Natl Acad Sci U S A***109**, E2794-2802 (2012).
42. Ashouri, J.F. & Weiss, A. Endogenous Nur77 Is a Specific Indicator of Antigen Receptor Signaling in Human T and B Cells. *The Journal of Immunology*, 1601301 (2016).
43. Cunningham, N.R. *et al.* Immature CD4 + CD8 + thymocytes and mature T cells regulate Nur77 distinctly in response to TCR stimulation. *J Immunol***177**, 6660–6666 (2006).
44. Nayar, R. *et al.* Graded levels of IRF4 regulate CD8 + T cell differentiation and expansion, but not attrition, in response to acute virus infection. *J Immunol***192**, 5881–5893 (2014).
45. Delgado, P., Fernández, E., Dave, V., Kappes, D. & Alarcón, B. CD3δ couples T-cell receptor signalling to ERK activation and thymocyte positive selection. *Nature***406**, 426–430 (2000).
46. Ryser, J.E., Rungger-Brändle, E., Chaponnier, C., Gabbiani, G. & Vassalli, P. The area of attachment of cytotoxic T lymphocytes to their target cells shows high motility and polarization of actin, but not myosin. *The Journal of Immunology***128**, 1159 (1982).
47. Cambi, A. *et al.* Organization of the Integrin LFA-1 in Nanoclusters Regulates Its Activity. *Molecular Biology of the Cell***17**, 4270–4281 (2006).
48. Roy, N.H. *et al.* LFA-1 signals to promote actin polymerization and upstream migration in T cells. *Journal of Cell Science***133**, jcs248328 (2020).
49. Au - Wabnitz, G., Au - Kirchgessner, H. & Au - Samstag, Y. Qualitative and Quantitative Analysis of the Immune Synapse in the Human System Using Imaging Flow Cytometry. *JoVE*, e55345 (2019).
50. Abrahamsen, G., Sundvold-Gjerstad, V., Habtamu, M., Bogen, B. & Spurkland, A. Polarity of CD4 + T cells towards the antigen presenting cell is regulated by the Lck adapter TSAd. *Sci Rep***8**, 13319–13319 (2018).
51. Blumenthal, D. & Burkhardt, J.K. Multiple actin networks coordinate mechanotransduction at the immunological synapse. *Journal of Cell Biology***219** (2020).
52. Opiela, S.J., Koru-Sengul, T. & Adkins, B. Murine neonatal recent thymic emigrants are phenotypically and functionally distinct from adult recent thymic emigrants. *Blood***113**, 5635–5643 (2009).

53. Fink, P.J. & Hendricks, D.W. Post-thymic maturation: young T cells assert their individuality. *Nature Reviews Immunology***11**, 544–549 (2011).
54. Thomas, P.G. *et al.* Physiological numbers of CD4 + T cells generate weak recall responses following influenza virus challenge. *J Immuno***184**, 1721–1727 (2010).
55. Turner, D.L. *et al.* Lung niches for the generation and maintenance of tissue-resident memory T cells. *Mucosal Immuno***7**, 501–510 (2014).
56. Thome, Joseph J.C. *et al.* Spatial Map of Human T Cell Compartmentalization and Maintenance over Decades of Life. *Cell***159**, 814–828 (2014).
57. Sathaliyawala, T. *et al.* Distribution and Compartmentalization of Human Circulating and Tissue-Resident Memory T Cell Subsets. *Immunity***38**, 187–197 (2013).
58. Schrum, A.G. Visualization of Multiprotein Complexes by Flow Cytometry. *Current Protocols in Immunology***87**, 5.9.1–5.9.14 (2009).
59. Reed, B.K. *et al.* A Versatile Simple Capture Assay for Assessing the Structural Integrity of MHC Multimer Reagents. *PLOS ONE***10**, e0137984 (2015).
60. Schrum, A.G. *et al.* High-sensitivity detection and quantitative analysis of native protein-protein interactions and multiprotein complexes by flow cytometry. *Sci STKE* 2007, pl2 (2007).

Figures

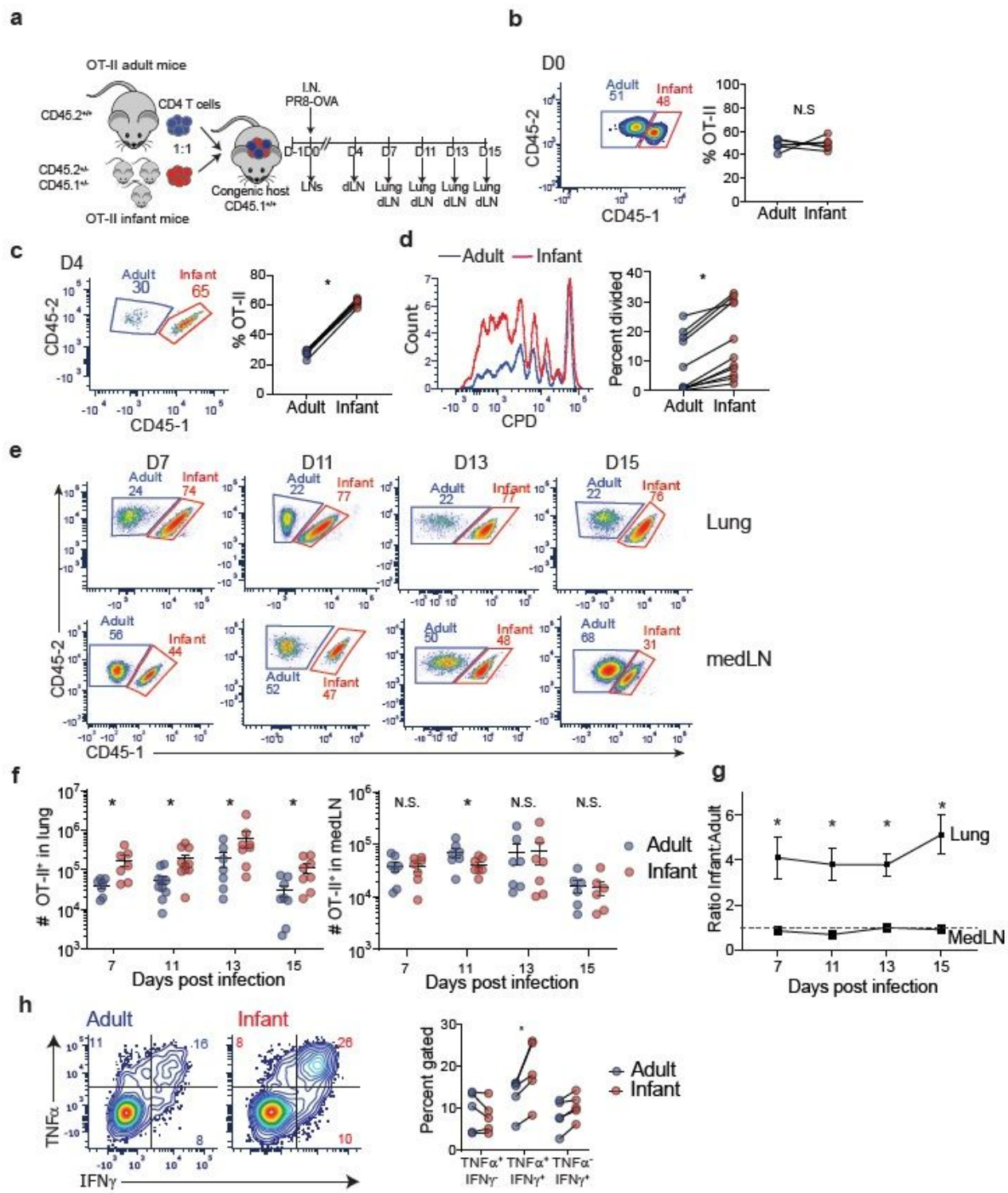


Figure 1

Enhanced generation of lung-homing effector cells by infant compared to adult T cells during respiratory virus infection. **a**, Schematic diagram depicting dual co-transfer of infant (red) and adult (blue) OT-II T cells into congenic host mice (CD45.2-/ CD45.1+/+), followed by infection with PR8-OVA one day post-transfer. Lungs and mediastinal draining lymph nodes (medLN) of hosts were harvested at indicated days post challenge. **b**, Frequency of transferred infant CD45.1+ (red) and adult CD45.1- (blue) OT-II cells

in LNs of host mice shown in representative flow cytometry plots (left) and in graphs of paired frequencies within individual host mice (right). c, MedLN T cells at day 4 post infection (p.i.) shown in representative flow cytometry plot (left) and graph with paired frequencies (right) of infant and adult OT-II cells in individual host mice after PR8-OVA infection. d, Enhanced proliferation by infant OT-II cells relative to adult OT-II cells in medLN of host mice shown by flow cytometry plots of CPD dilution (left) and paired frequencies of divided infant (red) and adult (blue) OT-II cells (right) in individual host mice. e, Infant T cells predominate in the lungs following infection. Representative flow cytometry plots showing frequency of infant (red) and adult (blue) OT-II effector cells from lungs and medLN of congenic hosts at indicated days post-infection. f, Increased numbers of infant lung T cells. Graphs showing total number of infant (red) and adult (blue) OT-II cells in lung (left) and medLN (right) of individual host at indicated days post infection. g, The ratio of OT-II infant to adult cell frequencies in lungs and medLN of congenic hosts post infection. h, Cytokine production by lung effector OT-II cells shown in representative flow plots of IFN- γ and TNF- α by infant and adult OT-II cells (left) and in graphs of paired frequencies of OT-II cells producing indicated cytokines from individual host mice (right). Data are representative of at least 2 independent experiments with $n = 3-4$ mice/experiment unless stated otherwise. Statistical analysis was done using student's t-test (paired) (* $p < 0.05$) with error bars representing standard error mean (S.E.M.).

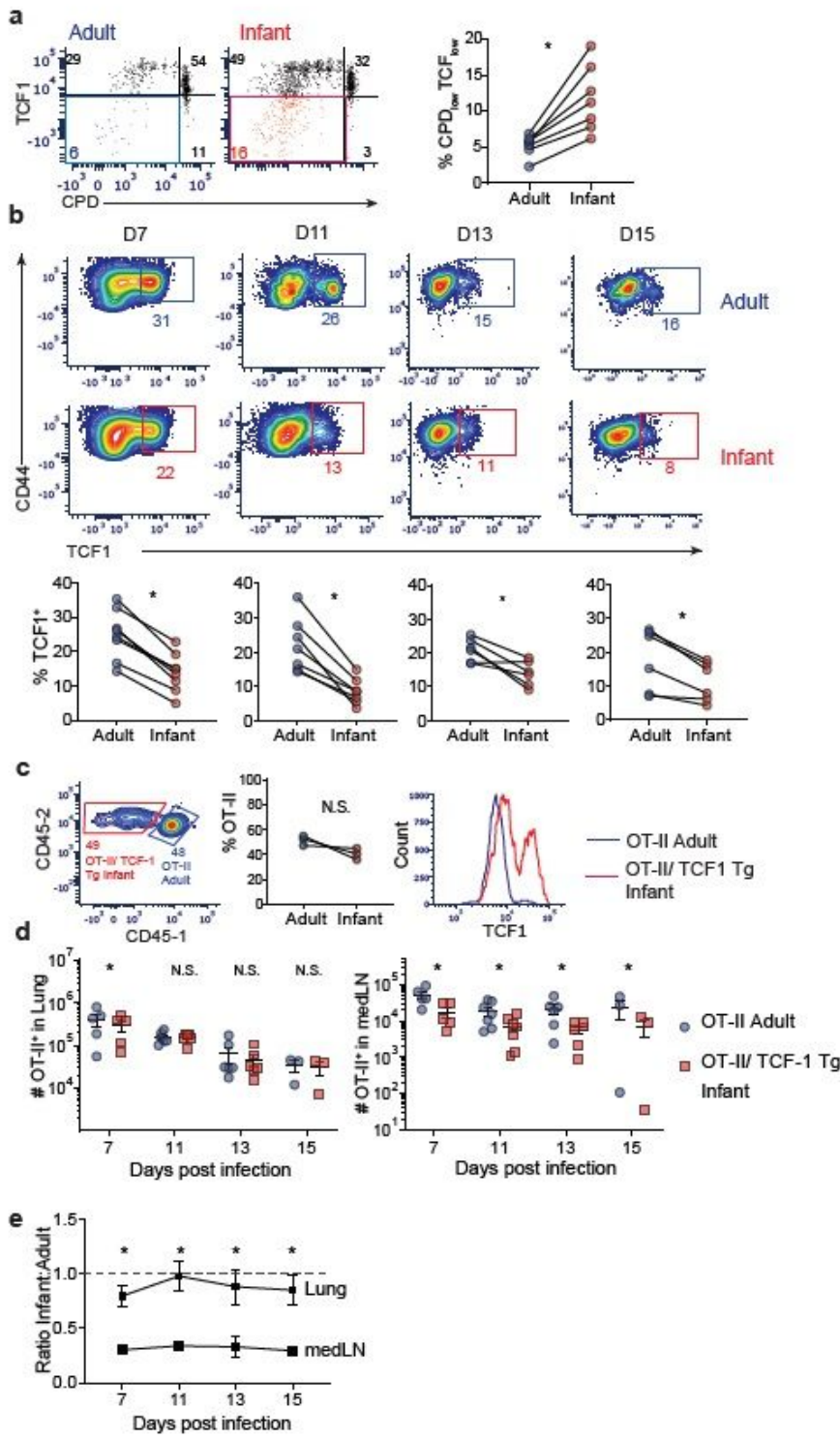


Figure 2

Infant T cells downregulate TCF-1 for enhanced proliferation but not effector generation. a, Expression of TCF-1 as a function of proliferation (CPD expression) at day 4 post infection in medLN of host mice shown in flow cytometry plots (left) and graphs of paired frequencies of (% CPD_{low} TCF_{flow}) infant and adult OT-II cells (right). b, TCF-1 expression shown in flow cytometry plots (top) and quantification of individual paired frequencies of TCF-1+ (bottom) in infant (red) and adult (blue) lung effector cells at

days indicated post challenge. c, Left: Representative flow cytometry plots of transferred infant OT-II/TCF-1 Tg CD45.1- (red) and adult CD45.1+ (blue) OT-II cells in LNs of host mice at day 0. Middle: Paired frequencies of infant and adult OT-II cells within individual host mice. Right: Higher baseline expression of TCF1 in OT-II/TCF-1 Tg infant (red) compared to adult (blue) cells in LNs at day 0. d, Total number of OT-II/TCF-1 Tg infant (red) and OT-II adult (blue) cells in lung (left) and medLN (right) of individual mice at indicated days post infection. e, The ratio of infant OT-II/TCF-1 Tg cells to adult OT-II cell frequencies in lung and medLN of congenic hosts at days indicated post infection. Data are representative of 2 independent experiments with $n = 3$ to 4 mice per experiment unless stated otherwise. Statistical analysis was done using paired Student's t-test.

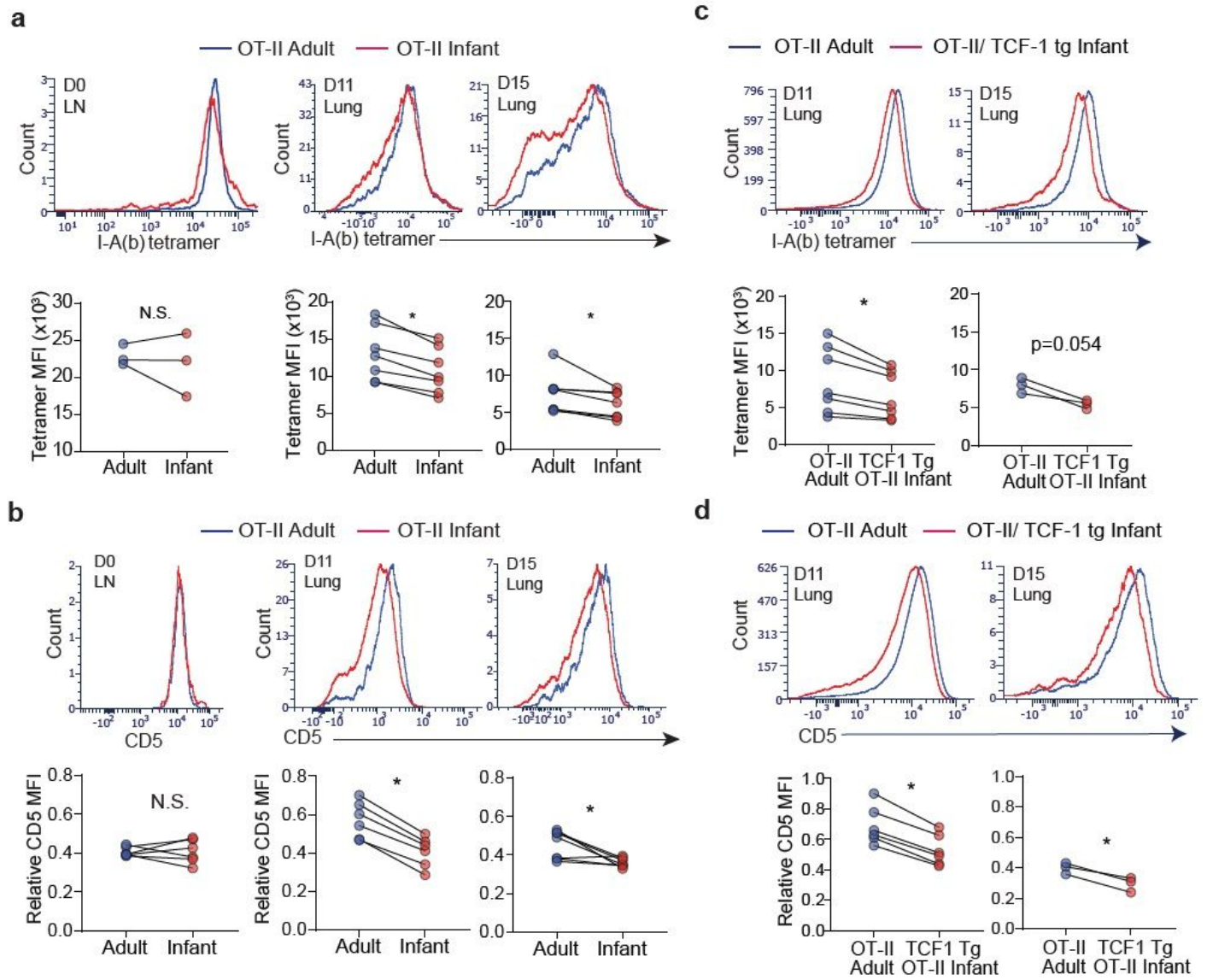


Figure 3

Infant T cells exhibit features of enhanced TCR-mediated signaling during influenza responses *in vivo*. a, Expression of OT-II TCR using I-A(b)AAHAEINEA tetramer on infant (red) and adult (blue) OT-II cells from LNs and lungs at indicated day p.i. shown in histograms (top) and graphs with mean fluorescent intensity

(MFI) of I-A(b) tetramer (bottom). b, Expression of CD5 on infant (red) and adult (blue) OT-II cells (top) and graphs showing the relative CD5 MFI (OT-II CD5 MFI to host CD4 naïve T cell CD5 MFI) (bottom) in LNs and lungs at indicated days p.i. c, Expression of OT-II TCR on lung infant OT-II/TCF-1 Tg and adult OT-II effector cells shown in representative flow cytometry plots (top) and graphs quantifying MFI of tetramer (bottom) of individual hosts. d, OT-II/TCF-1 Tg infant effector cells express lower levels of CD5 compared to adult effector cells as shown in flow cytometry plots (top) and graph with relative CD5 MFI on OT-II/TCF-1 Tg infant and adult OT-II cells (relative to CD5 MFI on host CD4 naïve T cells) (bottom) in LNs and lungs at indicated days p.i. Data are representative of 2 independent experiments with n = 3-4 mice per experiment unless stated otherwise. Statistical analysis was done using paired Student's t-test.

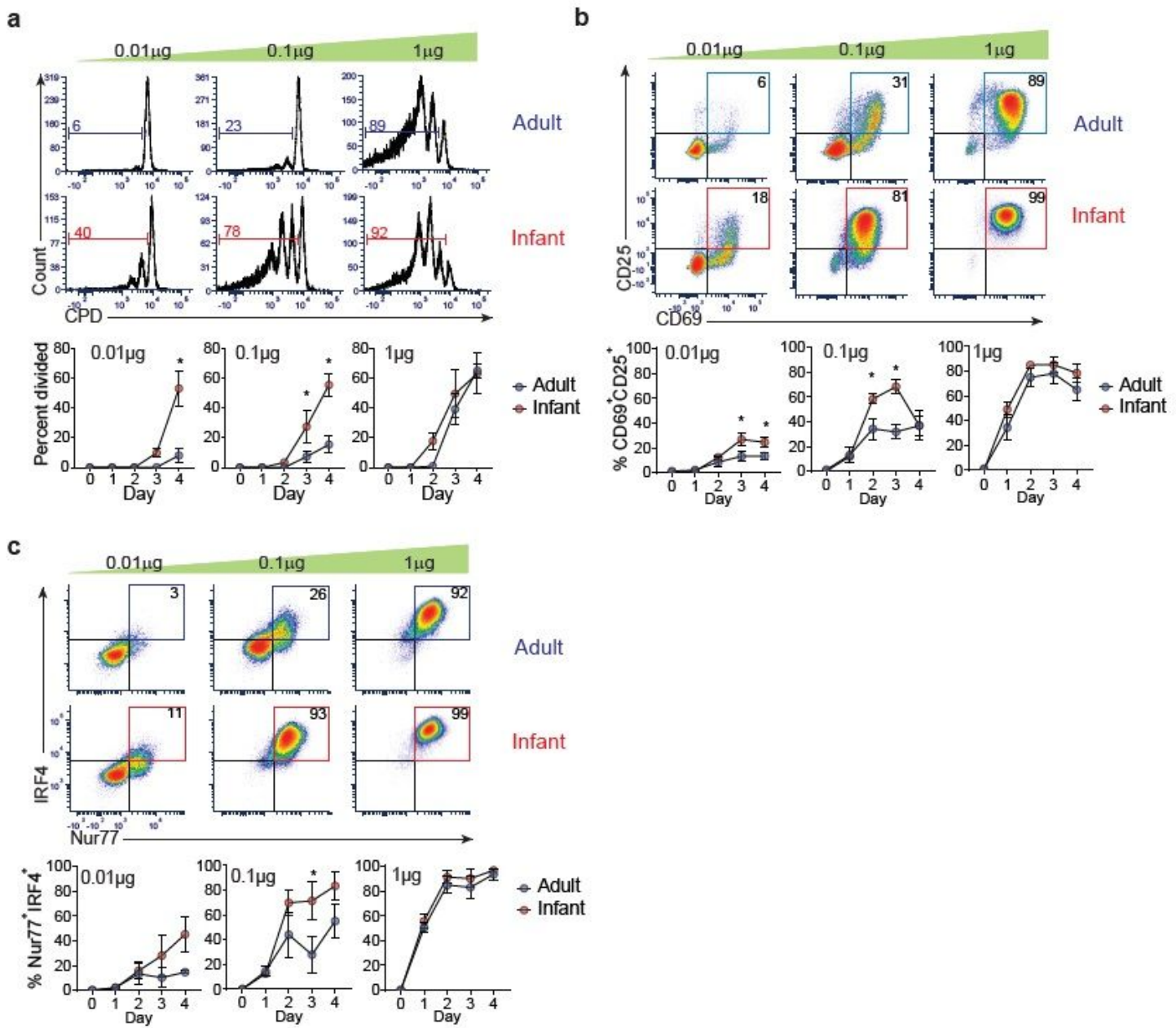


Figure 4

Infant T cells have enhanced TCR sensitivity leading to decreased activation threshold. a, Infant OT-II cells proliferate at lower doses of antigen with higher frequencies of cells divided compared to adult OT-II cells shown in representative flow cytometry plots (top) at day 3 post stimulation and graph quantifying percent of cells divided (bottom) at indicated dose and time. b, Expression of CD69 and CD25 on infant and adult OT-II cells upon stimulation shown in representative flow plots (top) at day 3 post stimulation and graph quantifying percent of CD69+CD25+ cells at the dose and time indicated (bottom). c, Expression of Nur77 and IRF4 on infant and adult OT-II cells upon stimulation shown in representative flow plot (top) at day 3 post stimulation and graph quantifying percent of Nur77+IRF4+ cells at the dose and time indicated (bottom). Data are compiled from 3 independent experiments. Significance was determined using Student's t-test.

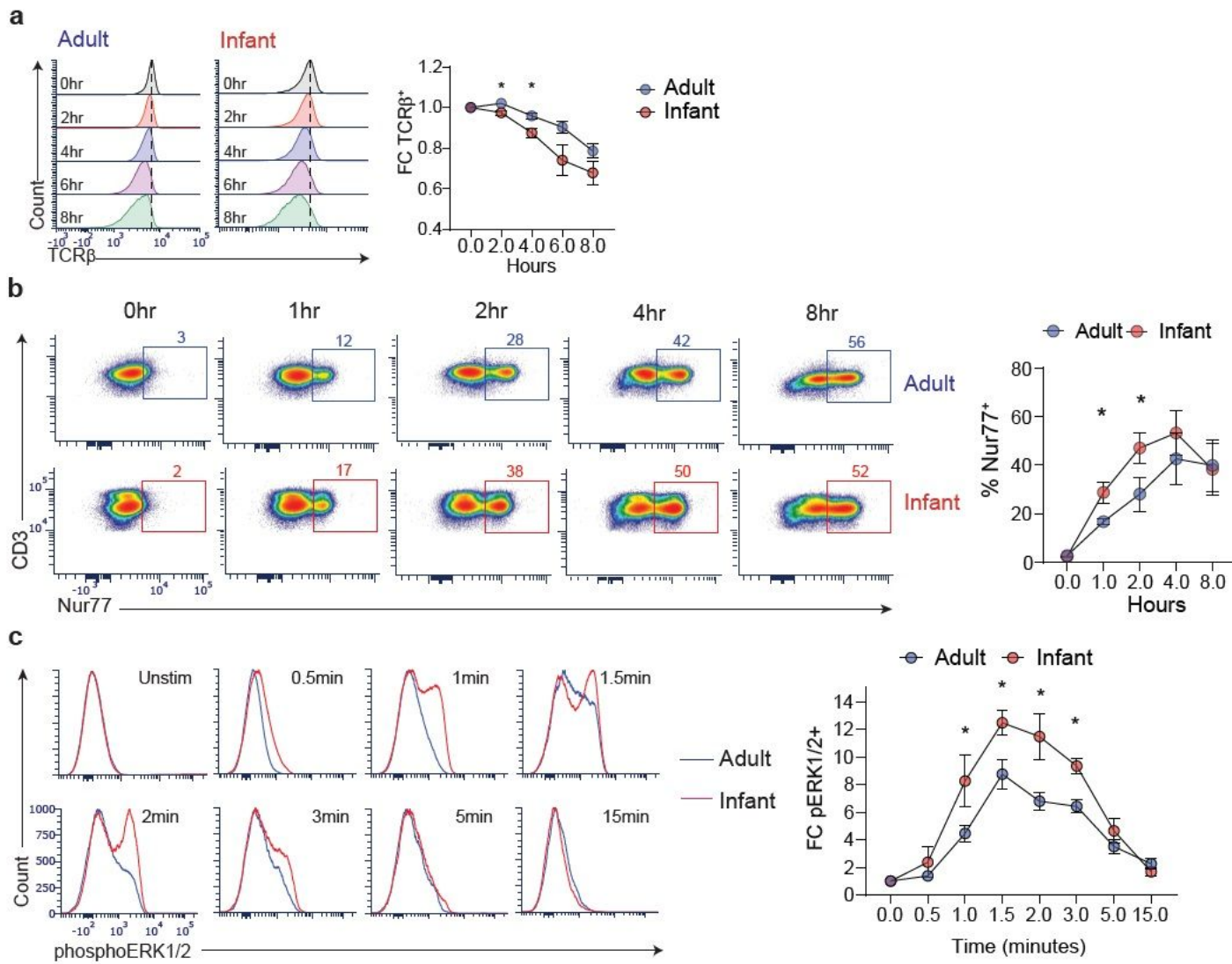


Figure 5

Increased proximal signaling by infant compared to adult T cells. a, Decreased expression of TCR- β on the surface of infant (red) compared to adult (adult) OT-II cells as shown in representative histograms (left) and graph showing fold change (FC) expression of TCR- β (bottom) upon stimulation relative to

unstimulated control. b, Expression of Nur77 in infant and adult OT-II cells shown in flow cytometry plots (left) and graph quantifying percent Nur77+ (right) in OT-II cells at times indicated upon stimulation. (a-b) Data shown is from 2 independent experiments with $n = 2$ in each experiment. Significance was determined using paired Student's t-test. c, Increased pERK1/2 expression upon TCR signaling in infant T cells compared to adult T cells shown in flow cytometric plots (left) and graph quantifying fold change (FC) in pERK1/2 expression relative to unstimulated controls (right) at times indicated upon stimulation. Data are compiled from 3 independent experiments. Significance was determined using two-way ANOVA with Sidak multiple comparison testing.

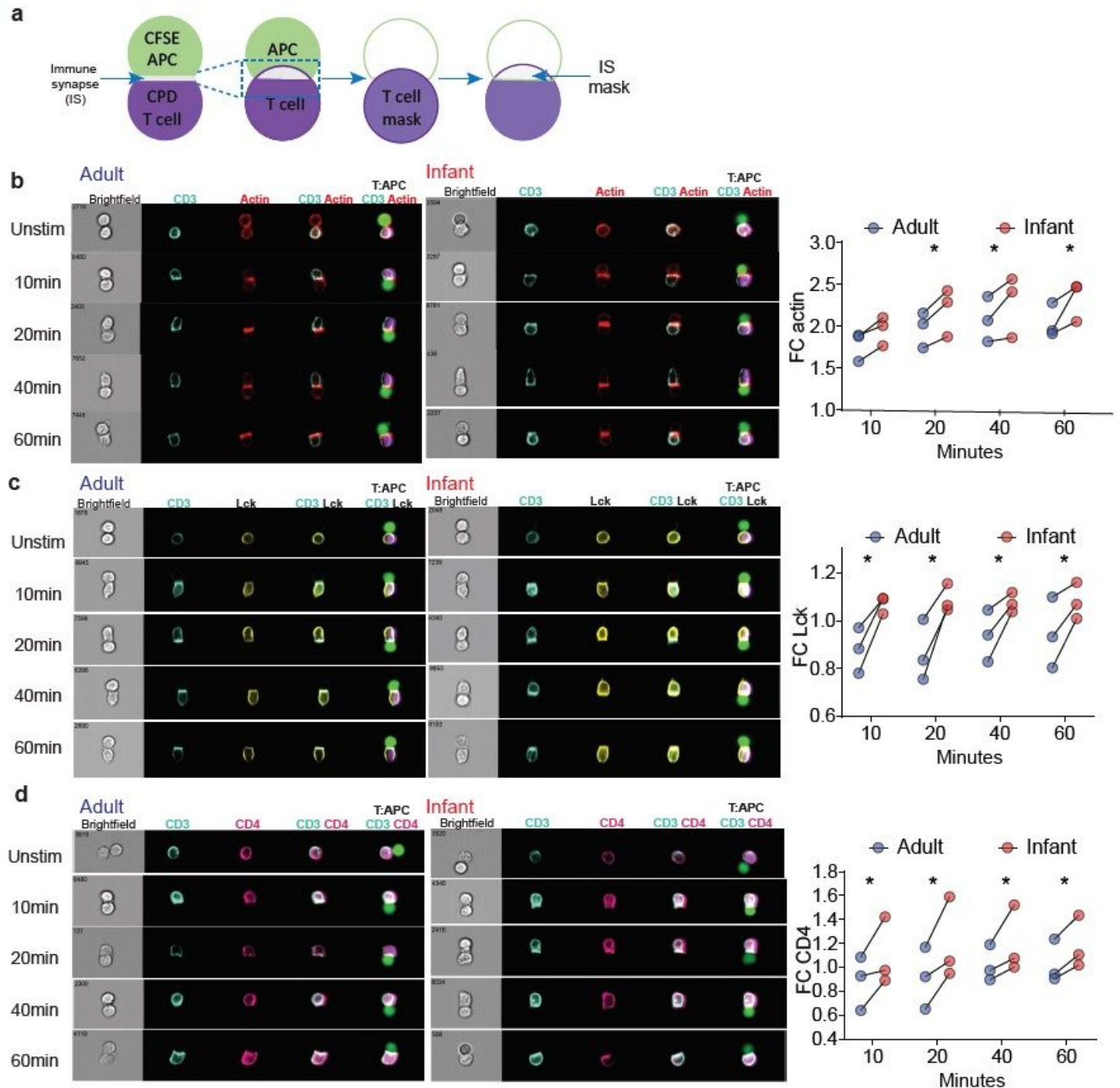


Figure 6

Infant T cells have higher accumulation of signaling molecule Lck, CD4, and actin on the immunological synapse (IS) compared to adult T cells. a, Schematic diagram of ImageStream analysis using IDEAS software to examine accumulation of actin, Lck, and CD4 in the immune synapse of conjugates upon stimulation (see methods). b, Infant T cells compared to adult T cells have higher accumulation of actin (red) with CD3 (turquoise) in T: APC conjugates as shown in representative images (left) and graph quantifying fold change (FC) relative to unstimulated control (right). c, Infant T cells compared to adult T cells have higher accumulation of Lck (yellow) with CD3 (turquoise) in T: APC conjugates as shown in representative images (left) and graph quantifying fold change (FC) relative to unstimulated control (right). d, Infant T cells compared to adult T cells have higher accumulation of CD4 (pink) with CD3 (turquoise) in T: APC conjugates as shown in representative images (left) and graph quantifying fold change (FC) relative to unstimulated control (right). Data are from 3 independent experiments.

Significance was determined using two-way ANOVA with Sidak multiple comparison testing.

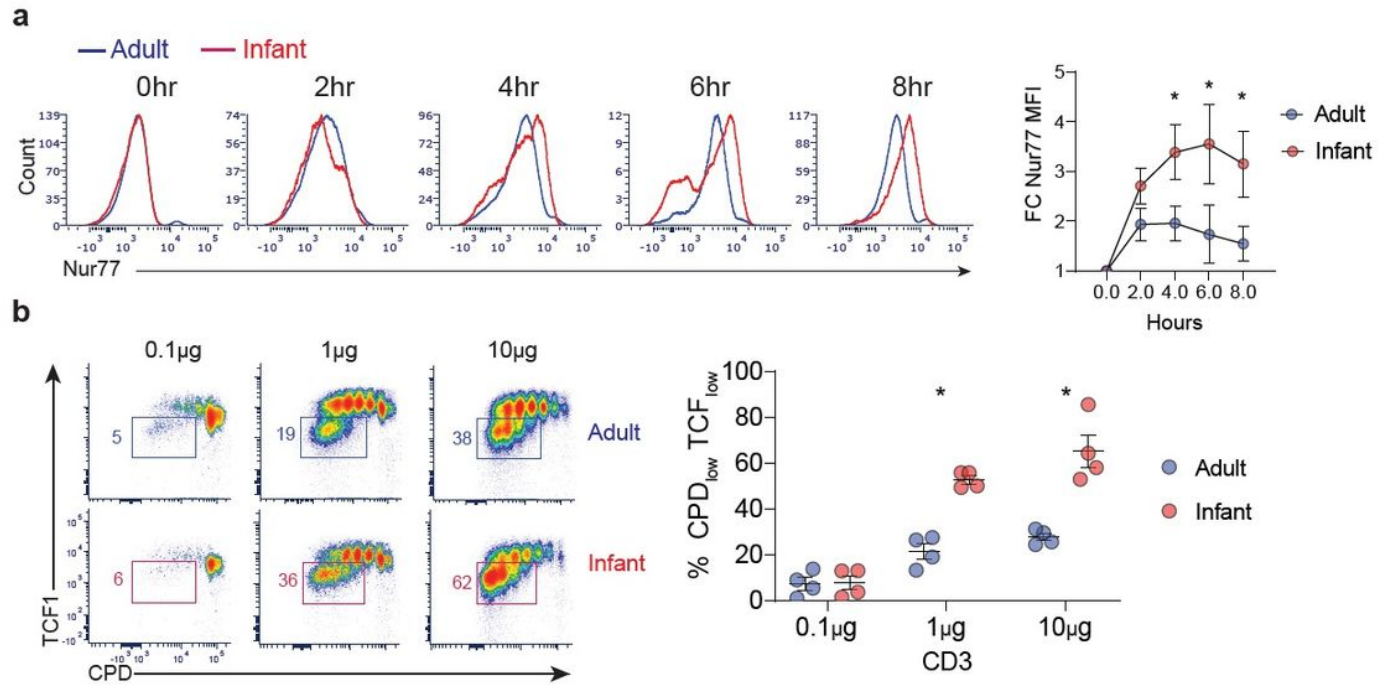


Figure 7

Human infant T cells exhibit early TCR-coupled signaling and enhanced TCF-1 downregulation. CD4 naive T cells from human infant and adult lymph nodes were stimulated with CD3/CD28/CD2 coated beads for time points indicated. a, Expression of Nur77 in human infant and adult T cells upon stimulation at times indicated shown in representative flow plots (left) and graph with fold change (FC) in expression of Nur77 (right) relative to unstimulated control. b, Expression of TCF1 as a function of proliferation (CPD expression) after 4 days of stimulation shown in flow cytometry plots (left) and graph with frequencies of infant (red) and adult (blue) T cells that downregulated TCF1 (right). Data are compiled from 3 independent experiments. Significance was determined using Student's t-test.

Supplementary Files

This is a list of supplementary files associated with this preprint. Click to download.

- [Supplementaltables.pdf](#)
- [supplementalfigures.pdf](#)
- [supplementalfigureV2.pdf](#)